Journal of Earthquake Engineering, Vol. 7, No. 1 (2003) 1–24

Imperial College Press
www.icpress.co.uk

PERFORMANCE-BASED DESIGN OF ADDED VISCOUS DAMPERS USING CAPACITY SPECTRUM METHOD

JINKOO KIM and HYUNHOON CHOI

Department of Architectural Engineering, Sungkyunkwan University, Chunchun-Dong, Jangan-Gu, Suwon, 440-746, Korea

KYUNG-WON MIN

Department of Architectural Engineering, Dankook University, San 8, Hannam-Dong, Yongsan-Gu, Seoul, 140-714, Korea

Received 15 May 2001
Revised 12 June 2002
Accepted 19 June 2002

The conventional practice of carrying out a series of trial and error process for design of supplemental dampers requires a lot of computation time and labour. In this study a straightforward design procedure for viscous dampers was developed based on capacity spectrum method in the context of performance based seismic design. The required amount of viscous damping to satisfy given performance acceptance criteria was evaluated from the difference between the overall demand for effective damping and the inherent damping plus the equivalent damping capacity of the structure originated from plastic deformation of each structural member. The proposed method was applied to single-degree-of-freedom systems with various design parameters such as natural period, yield strength, and the stiffness after the first yield. The procedure was also implemented to 10- and 20-storey steel frames for verification of the proposed method. According to the earthquake time history analysis results, the maximum displacements of the model structures with viscous dampers supplied in accordance with the proposed method correspond well with the given target displacements.

Keywords: Viscous dampers; capacity spectrum method; time history analysis; equivalent damping; performance-based seismic design.

1. Introduction

The ATC-40 document [1996] and the 1997 NEHRP's Guidelines [Federal Emergency Management Agency, 1997] propose technical strategies such as increasing strength, altering stiffness, and reducing demand by employing base isolation or energy dissipation devices to enhance seismic performance of a structure. Specifically the energy dissipation devices have advantage in improving structural performance without adding lateral forces associated with conventional strengthening schemes. They are especially effective in the velocity sensitive region of a response spectrum corresponding to the natural period between approximately 0.5–3 s, in which maximum acceleration of a structure decreases significantly as the damping in the structure increases.

The general procedure for seismic retrofit of a structure with supplemental dampers can be divided into the following steps: (1) Evaluate the seismic performance of the structure for the given levels of earthquake ground motion; (2) Determine the supplemental damping required to reduce the structural responses below the performance acceptance criteria; (3) Determine the proper damper size and locations to realise the desired damping ratio; (4) Analyse the structure-damper system to check the adequacy of the supplemental dampers. Tasks in Steps 1 and 4 can be conducted properly by nonlinear dynamic analysis, or by more simplified approximate methods. For example, FEMA-273 [1997] presents simplified nonlinear static procedure based on the capacity spectrum method (CSM) for evaluating the inelastic response of damper-added structure subjected to earthquake loads. The successful accomplishment of the second and the third steps, which are the key elements of the retrofitting process, largely depends on experience or on trial and error process. With the trial values for the dampers, the analytical process of Steps 4 is repeated until the proper amount and location of supplemental dampers to satisfy the given performance acceptance criteria are finalised. However, this conventional practice of carrying out series of trial and error process is quite a laborious task since the nonlinear static or dynamic analysis of structural systems with supplemental dampers requires a lot of computation time and labour. In this sense a more convenient but reliable method is needed in Steps 2 and 3 to reduce the overall design procedure, especially in the preliminary analysis and design stages.

In this study a systematic procedure based on CSM was developed focusing mainly on the Steps 2 and 3 of the design process. For Step 2, the amount of supplemental viscous damping required for an equivalent single-degree-of-freedom (SDOF) structure to satisfy the given performance acceptance criteria is obtained from the difference between the required overall damping obtained from the response spectrum and the hysteretic damping of the structure at the target displacement obtained from capacity curve. The design process can be conveniently carried out in the acceleration-displacement response spectrum (ADRS) coordinates without iteration or trial and error process. For Step 3, viscous dampers are distributed to each storey of the multi-degrees-of-freedom (MDOF) structure by equating the dissipated energy of the structure when it deforms to the target displacement, with the required damping obtained in Step 2.

It should be pointed out, however, that as the proposed procedure is based on CSM, it shares the same shortcomings inherent to the CSM. For example, Krawinkler [1995] pointed out that there is no physical principle that justifies the existence of a stable relationship between the hysteretic energy dissipation and the equivalent viscous damping, particularly for highly inelastic system. Fajfar [2000] stated that pushover analysis is based on a very restrictive assumption, i.e. a time-independent displacement shape, and it is in principle inaccurate for structures where higher mode effects are significant. Also for systems subjected to pulse-type near-field records, the proposed method may not be appropriate. Another limitation of the method is related to the modelling of the viscous dampers. For dampers

that the damping force is not linearly proportional to the velocity of the system, more rigorous dynamic analysis technique will be required.

2. Development of Design Procedure for Supplemental Viscous Dampers

2.1. *Modelling of viscous dampers*

The viscous dampers have advantage in providing damping without changing dynamic modal characteristics. It is stated in FEMA-274 [1997] that the damping force provided by viscous dampers can be modelled to be proportional to the velocity with constant exponent ranging from 0.5 to 2.0. In preliminary analysis and design stage, the velocity exponent of 1.0 is generally recommended for simplicity [Soong and Dargush, 1997]. Therefore in this study the damping force produced by viscous dampers were considered to be proportional to the velocity with a constant velocity exponent of 1.0 (linear dashpot) for convenience.

2.2. *Lateral load distribution for pushover analysis*

The first step for application of CSM is to transform the structure to an equivalent SDOF structure. Proper guidelines are provided in references [ATC, 1996, for example]. It also requires that both the demand spectra and structural capacity curve be plotted in the spectral acceleration S_a vs. spectral displacement S_d domain, which is known as the acceleration-displacement response spectra (ADRS) [ATC, 1996]. To convert a response spectrum with the standard acceleration *vs.* natural period format to ADRS, it is necessary to determine the value of S_d corresponding to each point on the original curve. The relationship between the base shear and the top storey displacement, which is generally called pushover curve or capacity curve [Freeman, 1998], is obtained by gradually increasing the lateral loads appropriately distributed over the storeys. There are many alternatives for the distribution of the lateral loads, and it may be expected that different patterns of lateral loads result in pushover curves with different characteristics and different sequence of plastic hinge formation. In this study the capacity curve was obtained by applying three different patterns of lateral seismic loads:

(1) Forces are applied in proportion to the product of storey masses and the fundamental mode shape of the elastic model structure [ATC, 1996]:

$$F_i = \frac{m_i \phi_{i1}}{\sum_{i=1}^{N} m_i \phi_{i1}} V \tag{2.1a}$$

where F_i is the seismic storey force in the ith floor, m_{i1} is the mass of the ith floor, ϕ_i is the ith component of the mode shape vector for the fundamental mode, V is the base shear, and N is the number of floors.

(2) The effect of the higher modes is considered by means of combination of modes using SRSS (square root of sum of squares) method [Freeman *et al.*, 1998]:

$$F_i = \sqrt{\sum_{j=1}^{N} \left(\frac{\sum_{i=1}^{N} m_i \phi_{ij}}{\sum_{i=1}^{N} m_i \phi_{ij}^2} \phi_{ij} S_{aj} m_i \right)^2} \tag{2.1b}$$

where ϕ_{ij} is the ith component of the jth mode shape vector and S_{aj} is the spectral acceleration corresponding to the jth mode.

(3) Equivalent mode shape considering modal participation factors for higher modes is utilised [Valles *et al.*, 1996]:

$$F_i = \frac{m_i \bar{\phi}_i}{\sum_{i=1}^{N} m_i \bar{\phi}_i} V \tag{2.1c}$$

where $\bar{\phi}_i = \sqrt{\sum_{i=1}^{n} (\phi_{ij} \Gamma_j)^2}$ and $\Gamma_j = \frac{\sum_{i=1}^{N} m_i \phi_{ij}}{\sum_{i=1}^{N} m_i \phi_{ij}^2}$.

The first method can be properly applied to a structure in which the first mode dominates the dynamic motion. The second and the third methods have advantage that higher mode effect can be included in the estimation of the lateral seismic loads.

2.3. *Effective damping of a yielding structure with supplemental dampers*

The equivalent viscous damping ratio for the yielding structure is determined from the energy dissipated by the hysteretic behaviour, E_D, which is the area enclosed by the hysteresis loop at maximum displacement, and the stored potential energy corresponding to the area of the shaded triangle, E_S, as shown in Fig. 1 [Chopra, 1995; FEMA, 1997]:

$$\beta_{\text{eq}} = \frac{1}{4\pi} \frac{E_D}{E_S} = \frac{2(S_{ay} S_{dp} - S_{dy} S_{ap})}{\pi S_{dp} S_{ap}} \tag{2.2}$$

where the variables S_{ay} and S_{dy} are the acceleration and displacement of the equivalent SDOF system at yield. A bilinear representation of the capacity spectrum, as described in Fig. 1, is needed to estimate the effective damping and appropriate reduction of spectral demand. ATC-40 recommends that the area under the original capacity curve and the equivalent bilinear curve be equal so that the energy associated with each curve is the same. If the inherent viscous damping of the structure is assumed to be β, then the effective damping ratio of the system can be obtained as

$$\beta_{\text{eff}} = \beta + \kappa \beta_{\text{eq}} \tag{2.3}$$

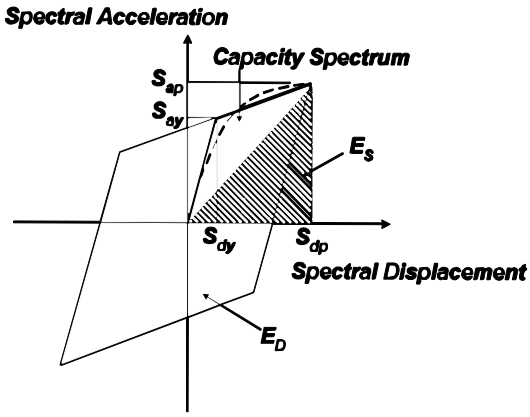

Fig. 1. Estimation of equivalent damping ratio.

where κ is the efficiency factor or damping modification factor which is equal to the actual area enclosed by the hysteresis loop divided by the loop area of the corresponding perfect bilinear hysteretic system [ATC, 1996; FEMA, 1997]. In this study the factor is taken to be 1.0 because perfect bilinear system is assumed in the analysis. The effective damping is used to plot the demand curve.

When additional energy dissipation devices are added, the effective damping becomes [FEMA-274, 1997]:

$$\beta_{\text{eff}} = \frac{1}{4\pi}\frac{E_{DE}/m + E_{DS}}{E_S} + \beta \tag{2.4}$$

where E_{DE} is the energy dissipated by the dampers and m is the effective mass of the system. The first term in the right hand side represents the equivalent damping contributed from the added dampers. The energy dissipated by viscous dampers for a cycle of harmonic motion can be computed as follows:

$$E_{DE} = \pi c \omega S_{dp}^2 = 2\pi\beta_v \frac{T_{\text{eff}}}{T} k_{\text{eff}} S_{dp}^2 \tag{2.5}$$

where c is the damping coefficient of a linear viscous damper, ω and ω_{eff} are the forcing and effective frequencies, respectively, k_{eff} is the effective stiffness of the system, and β_v is the damping ratio of the system with viscous dampers vibrating harmonically at effective period. In this study the forcing frequency is assumed to be the same with the elastic natural frequency of a structure. If Eq. (2.5) is substituted to Eq. (2.4), then the overall effective damping including the contribution from the dampers can be obtained [Tsopelas *et al.*, 1997]:

$$\beta_{\text{eff}} = \beta_{\text{eq}} + \beta + \beta_v \frac{T_{\text{eff}}}{T_e} \tag{2.6}$$

where T_e is the effective elastic period, and the relations $\omega_{\text{eff}}^2 = k_{\text{eff}}/m$, $S_{ap} = \omega_{\text{eff}}^2 S_{dp}$ were utilised in the formulation.

2.4. *Supplemental damping required to meet the performance criterion*

Equation (2.6) represents the total effective damping of the system with added dampers, which can be used in the evaluation of structural response to reduce the demand spectrum accounting for the effect of the dampers. When a desired target response is predetermined, as in the case of seismic retrofit, the amount of supplemental damping, β_v, required to be supplied to meet a given performance criterion, can be obtained by transforming Eq. (2.6) to the following form:

$$\beta_v = (\beta_{\text{eff}} - \beta - \beta_{\text{eq}})\frac{T_e}{T_{\text{eff}}}\,. \tag{2.7}$$

The difference of Eq. (2.7) from Eq. (2.6) is that the effective damping is obtained directly from the demand spectrum which crosses the capacity spectrum at the given target point (S_{dT}, S_{aT}). The equivalent damping is evaluated at the given target point. The procedure for evaluation of the required additional viscous damping is as follows:

(1) Obtain bi-linear capacity spectrum in ADRS format from pushover curve. The effective elastic stiffness k_e and the effective elastic period T_e can be computed in this stage.
(2) Determine the target displacement, S_{dT}, that satisfies the given performance objective.
(3) Evaluate the equivalent damping from the capacity spectrum by reading the spectral ordinates (S_{dT}, S_{aT}) and computing the effective period $T_{\text{eff}} = 2\pi\sqrt{S_{dT}/S_{aT}}$.
(4) Obtain in the ADRS the damping ratio, β_{eff}, of the demand spectrum that crosses the capacity spectrum at the target displacement. This corresponds to the overall demand of damping required for the structure to meet the given performance objective.
(5) The viscous damping that must be supplemented to limit the maximum displacement within the target displacement, β_v, can be obtained from Eq. (2.7).

The key point in the above procedure is that the effective damping (demand from earthquake) and the equivalent damping (capacity of the structure) are obtained at the given target displacement, and the difference between them is provided by the supplemental dampers. It should be pointed out that even though Eq. (2.7) was obtained from simple modification of Eq. (2.6), the implication is quite different. It will be shown later that the proposed procedure reduces the design process and computation time significantly since the required supplemental damping is obtained in a single design process without iteration or trial and error process.

2.5. *Distribution of supplemental dampers in MDOF system*

In a SDOF system the additional damping required to meet the target displacement can simply be added to the system. In a multi-storey structure, however, the damping should properly be distributed over the storeys. To this end Eq. (2.2) is used again. If the dampers are placed as diagonal members with the inclination θ as shown in Fig. 2, then the energy dissipated by the dampers and stored in the structure can be expressed as follows as in [FEMA-274] [1997]

$$E_{DE} = \frac{2\pi^2}{T} \sum_j C_j \cos^2 \theta_j (\Delta_i - \Delta_{i-1})^2 \tag{2.8a}$$

$$E_S = \frac{2\pi^2}{T^2} \sum_j m_j \Delta_j^2 \tag{2.8b}$$

where T is the fundamental natural period of the structure, C_j and Δ_j are the damping coefficient and the maximum lateral displacement of the jth storey, respectively. By substituting Eq. (2.8) into Eq. (2.2), the damping ratio contributed from the dampers can be obtained as

$$\beta_v = \frac{T \sum_i C_i \cos^2 \theta_i (\Delta_i - \Delta_{i-1})^2}{4\pi \sum_i m_i \Delta_i^2} \tag{2.9}$$

where m_i is the mass of the ith storey. For the given displacement shape and the required damping ratio, the appropriate damping coefficient for each storey, C_i, can be identified. In the design process, however, the maximum lateral displacements are unknown in this stage. Therefore later in this study various configurations for lateral storey drifts are implemented in Eq. (2.9) to find out the most effective storey-wise distribution of viscous dampers. One of the simplest case will be to use the same amount of dampers in every storey, and to assume that the maximum

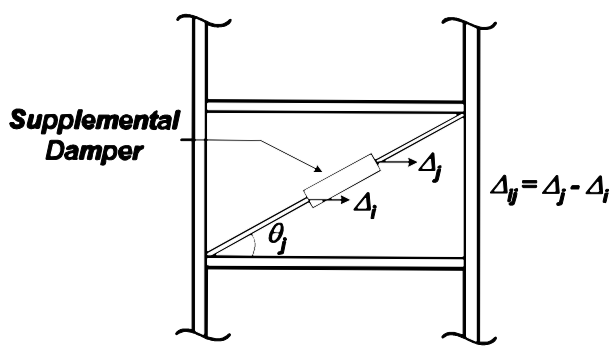

Fig. 2. Relative displacement of a supplemental damper.

storey drifts are proportional to the fundamental mode shape vector or to the pushover curve.

3. Application to SDOF Systems

The proposed procedure was applied to SDOF systems with various natural periods, strength ratios, and the post-yield stiffness ratios. To obtain more generalised results the mean response spectra constructed from as many as 20 horizontal earthquake records were used in the evaluation of the performance points using CSM. The target displacement of a structure with each parameter set was arbitrarily set to be 80% of the maximum displacement of the structure. Then the required viscous damping needed to restrain the structures within the target point was estimated using Eq. (2.7). Finally the maximum responses of the structures installed with the supplemental dampers were computed by nonlinear time history analyses, and the results were compared with the target values to check the accuracy of the proposed method.

3.1. *Model structures*

All of 12 SDOF systems with the following design parameters were analysed:

(1) Elastic period: $T_e = 0.1$, 1.0 and 2.0 s.
(2) Ratio of yield strength and the strength of the corresponding linear system: $e = 0.1$ and 0.5
(3) Post-yield to initial stiffness ratio: $\alpha = 0.05$ and 0.3.

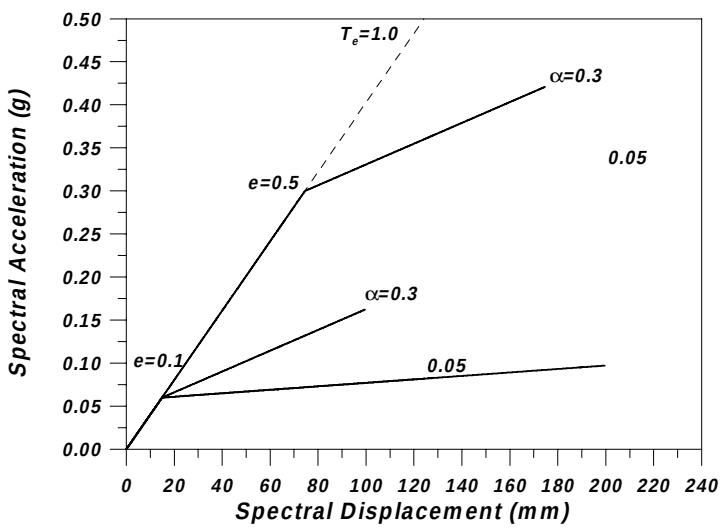

Fig. 3. Capacity spectra of the model structures ($T_e = 1.0$).

The elastic period was varied by modifying stiffness while mass was kept constant of a unit value. The capacity spectra for the model structures are presented in Fig. 3.

3.2. *Input seismic loads*

For numerical analysis 20 earthquake records, listed in Table 1, were taken from the Strong Motion Database of UC, Santa Barbara and PEERC (Pacific Earthquake Engineering Research Center). Each of these earthquakes has a magnitude larger than 6.5, an epicentral distance farther than 10 km, and site conditions of soft rock to stiff soil. The records were scaled in such a way that the frequency content of each record was preserved and an equal contribution of these records to the mean response spectrum was ensured. The detailed process of scaling can be found in the references [Tsopelas *et al.*, 1997; FEMA, 1997]. Figure 4(a) shows the 10% damped demand spectra for the 20 scaled motions, together with the mean spectrum. Figure 4(b) presents the mean response spectra for various damping ratios, which are later converted to the ADRS format together with the capacity spectrum to obtain the performance point.

3.3. *Evaluation of performance points*

The general procedure of CSM presented in ATC-40 was followed to analyse the model structures (without dampers). To obtain the maximum displacement using

Table 1. Earthquake records used in the parametric study.

Earthquake (Year)	Station	Magnitude	Comp.	PGA (cm/s^2)	PGV (cm/s)
W. Washington (1949)	325	7.1	N04W	161.6	21.4
			N86E	−274.6	−171.1
Eureka (1954)	022	6.5	N11W	164.5	−31.6
			N79E	−252.7	29.4
San Fernando (1971)	241	6.6	N00W	−250.0	−29.8
			S90W	−131.7	23.8
	458	6.6	S00W	113.9	31.8
			S90W	103.5	−28.6
Loma Prieta (1989)	Gilroy 2	7.1	90	316.3	−39.2
			0	344.2	33.3
	Hollister	7.1	90	−174.5	−30.9
			0	361.9	62.8
Landers (1992)	Yermo	7.5	360	−148.6	29.0
			270	−240.0	50.8
	Joshua	7.5	90	278.4	−42.7
			0	268.3	27.5
Northridge (1994)	Moorpark	6.7	180	286.2	20.3
			90	189.3	20.4
	Century	6.7	90	250.7	21.4
			360	217.6	25.1

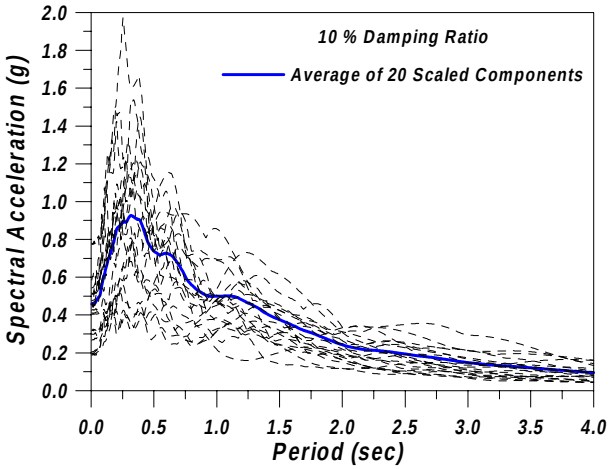

(a) Response spectra for 10% damping

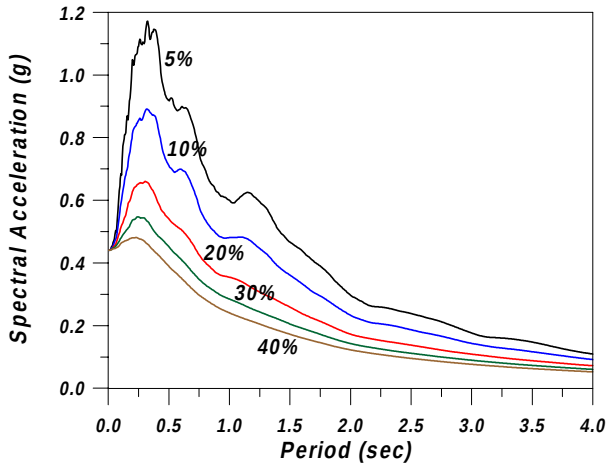

(b) Mean spectra for various damping

Fig. 4. Response spectra for the 20 earthquake records.

CSM, the response spectra shown in Fig. 4 are transformed to the demand spectra in ADRS format as shown in Fig. 5. Then the capacity spectra of model structures are also plotted in the same figure. From the intersection of the demand and capacity spectra the first trial value for the maximum displacement and acceleration of one of the model structure can be found. Then based on the performance point the new trial value for the effective damping ratio is estimated from Eq. (2.3). The demand spectrum is modified using the new effective damping ratio, and a new performance point is found from the intersection with the capacity spectrum. This process is repeated until the equivalent damping computed from the maximum

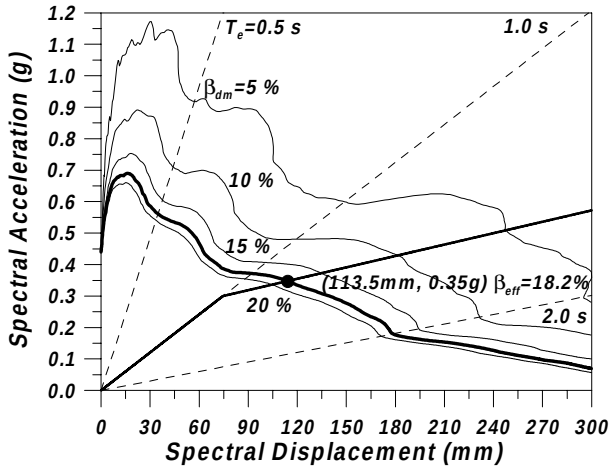

Fig. 5. Evaluation of the performance point in ADRS format.

response plus the inherent damping becomes very close to the effective damping of the demand spectrum that crosses the capacity spectrum at the performance point.

For verification of the responses obtained from the static procedure, nonlinear dynamic time history analyses (THA) were carried out for each model structure using the 20 scaled earthquake records. These analyses were performed using the program NONSPEC [Mahin *et al.*, 1983]. The mean values were compared with the responses computed from CSM. Table 2 describes the process of determining maximum response for a model structure with $T_e = 1.0$, $e = 0.5$, and $\alpha = 0.3$ as an example. In the table, S_{dy} and S_{ay} are the displacement and acceleration at yield, and S_{di} and S_{ai} represent the maximum responses obtained at each trial. The same procedures were repeated for all model structures, and the results were summarised in Table 3. It can be noticed that the displacements of the structures with the yield strength ratio $e = 0.5$ computed from CSM are generally smaller than those from time history analysis, and that the opposite is true when $e = 0.1$.

Table 2. Evaluation of performance points for structure with $T_e = 1.0$, $e = 0.5$, and $\alpha = 0.3$.

β_{dm} (%)	S_{dy} (mm)	S_{ay} (g)	S_{di} (mm)	S_{ai} (g)	β_{eff} (%)
5			247.56	0.51	23.3
10			181.45	0.43	23.3
15	74.52	0.30	134.70	0.37	21.0
20			104.48	0.34	15.8
:			:	:	:
18.2			113.52	0.35	18.2

(β_{dm}: damping ratio, S_{dy}: yield displacement, S_{ay}: acceleration at yield, S_{di} and S_{ai}: performance points, β_{eff}: effective damping.)

Table 3. Maximum displacements of model structures.

T_e	e	α	S_{dy}	D_{CSM}	D_{THA}	$D_{\mathrm{CSM}}/D_{\mathrm{THA}}$
0.1	0.5	0.3	1.12	1.78	1.98	0.90
		0.05		2.57	3.05	0.84
	0.1	0.3	0.23	5.57	5.09	1.09
		0.05		32.72	28.58	1.14
1.0	0.5	0.3	74.52	113.52	129.87	0.87
		0.05		104.37	133.83	0.78
	0.1	0.3	14.91	184.30	164.79	1.12
		0.05		148.85	174.33	0.85
2.0	0.5	0.3	149.05	208.29	243.45	0.86
		0.05		197.13	256.61	0.77
	0.1	0.3	29.81	279.18	281.98	0.99
		0.05		203.72	260.79	0.78

(T_e: elastic period, e: strength ratio, α: post-yield stiffness ratio, S_{dy}: displacement at yield, D_{CSM}: displacement from CSM, D_{THA}: displacements from time history analysis, unit: mm.)

It also can be observed that the difference between the results of the two analysis methods is larger when the post-yield stiffness of the system is small ($\alpha = 0.05$). The results presented in Table 3 are compared graphically in Fig. 6, where the ratios of the maximum displacements computed from CSM and dynamic analysis are plotted. As mentioned above, it can be found that the ratio deviates from 1 as the post-yield stiffness decreases. Nevertheless, for the given conditions, it can be concluded that the results from the CSM generally corresponds well with those from the THA regardless of the variation of the design parameters.

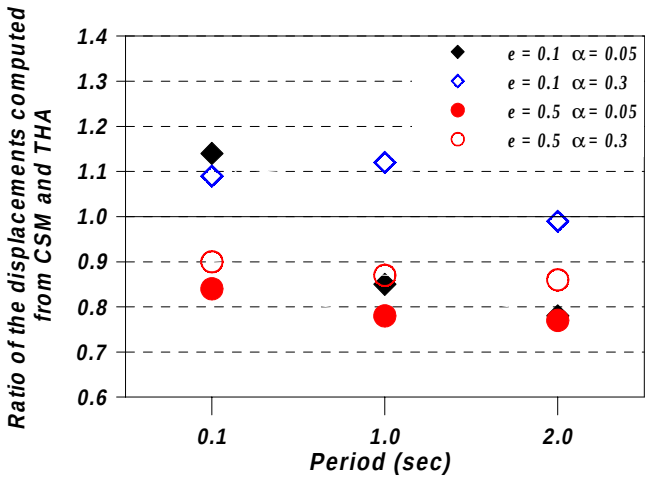

Fig. 6. Ratios of analysis results and target displacements for various stiffness ratios (e: yield strength ratio, α: strain hardening ratio).

Table 4. Procedure for estimating required supplemental damping.

T_e	e	α	D_{TG} (mm)	β_{eq} (%)	β_{eff} (%)	β_v (%)	D_{THA} (mm)	$D_{\mathrm{THA}}/D_{\mathrm{TG}}$
0.1	0.5	0.3	1.42	8.9	28.0	13.0	1.51	1.06
		0.05	2.05	26.5	40.1	6.5	2.30	1.12
	0.1	0.3	4.45	6.3	19.4	4.7	4.21	0.94
		0.05	26.17	8.8	18.6	1.2	23.90	0.91
1.0	0.5	0.3	90.81	7.5	22.9	9.8	96.02	1.06
		0.05	83.49	6.5	25.8	13.5	82.36	0.99
	0.1	0.3	147.44	10.9	22.0	3.7	136.46	0.93
		0.05	119.08	39.2	55.9	4.8	145.16	1.22
2.0	0.5	0.3	166.63	4.6	22.8	12.7	175.15	1.05
		0.05	157.70	3.3	25.0	16.3	165.64	1.05
	0.1	0.3	223.34	13.1	26.1	5.0	226.48	1.01
		0.05	162.97	40.4	62.7	8.2	205.94	1.26

(D_{TG}: target displacements, and D_{THA}: displacements form THA, β_{eq}: equivalent damping, β_{eff}: effective damping, β_v: required supplemental damping.)

3.4. *Evaluation of the required supplemental damping*

The supplemental damping ratios required to restrain the structures within the target displacements were computed following the process described in Sec. 2.4, and the maximum displacements of the model structures with the supplemental dampers were computed using THA. The results are summarised in Table 4, in which it can be seen that the maximum displacements of the model structures, D_{THA}, generally match well with the target displacements, D_{TG}; in most cases the error is less than 10%. As the target displacements were set to be 80% of the maximum displacements obtained from the CSM, the accuracy of the proposed method largely depends on that of the CSM itself; i.e. for cases that the results from the CSM and the THA coincide well, the maximum displacements of the structures with added damping are very close to the target displacements. This can be verified by comparing the last columns of Table 3 and Table 4. Also it can be found that the system with small post-yield stiffness ratio α (i.e. system with large ductility demand) requires smaller supplemental damping, which is natural considering the fact that the equivalent damping due to inelastic deformation generally increases as the yield strength decreases (i.e. as the ductility demand increases). On the whole it can be concluded that in SDOF systems the proposed method can provide the amount of required supplemental damping precisely for given target displacement.

4. Application of the Proposed Process to Multi-Storey Structures

4.1. *Model structures*

The 10-storey and 20-storey model frames for analysis, shown in Fig. 7, were utilised for application of the proposed process. The 10-storey structure was designed to resist gravity and wind load, while the 20-storey structure was designed

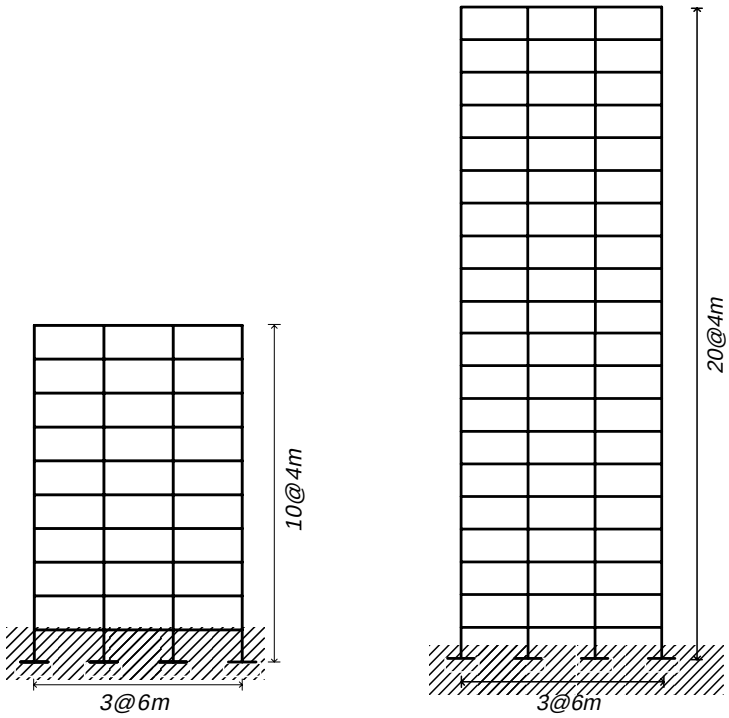

(a) 10-storey structure (b) 20-storey structure

Fig. 7. Model structures for implementation of the proposed method.

Table 5. Sectional properties of model structures.

Model	Levels	Columns		Beams
		Interior Columns	Exterior Columns	
10-storey	$8 \sim 10$	H344 × 354 × 16 × 16	H298 × 299 × 9 × 14	H350 × 175 × 7 × 11
	$5 \sim 7$	H350 × 350 × 12 × 19	H300 × 300 × 10 × 15	H396 × 199 × 7 × 11
	$1 \sim 4$	H400 × 400 × 13 × 21	H344 × 348 × 10 × 16	H400 × 200 × 8 × 13
20-storey	$17 \sim 20$	H394 × 398 × 11 × 18	H344 × 354 × 16 × 16	H400 × 200 × 8 × 13
	$13 \sim 16$	H400 × 400 × 13 × 21	H350 × 350 × 12 × 19	H446 × 199 × 8 × 12
	$9 \sim 12$	H406 × 403 × 16 × 24	H394 × 398 × 11 × 18	H450 × 200 × 9 × 14
	$5 \sim 8$	H414 × 405 × 18 × 28	H400 × 400 × 13 × 21	H496 × 199 × 9 × 14
	$1 \sim 4$	H428 × 407 × 20 × 35	H406 × 403 × 16 × 24	H500 × 200 × 10 × 16

Table 6. Dynamic characteristics of the model structures.

Model	Mode	1	2	3	4	5
10-storey	Period (s)	1.41	0.49	0.28	0.19	0.14
	Modal Participation Factor	1.34	0.51	0.30	0.22	0.16
	Effective Mass (%)	77.54	11.68	4.28	2.23	1.53
20-storey	Period (s)	3.24	1.12	0.65	0.45	0.34
	Modal Participation Factor	1.37	0.56	0.32	0.22	0.17
	Effective Mass (%)	74.71	13.02	4.24	2.27	1.46

only for gravity load to make it more flexible. For gravity load uniform dead load of 540 kgf/m^2 and live load of 250 kgf/m^2 were applied throughout the storeys. Basic wind speed of 35 m/s was used for lateral static wind load. The yield stress of the structural steel is 2.4 tonf/m^2 and 3.3 tonf/m^2 for beams and columns, respectively. The structural analysis and design were carried out using the program MIDAS-GEN [POSCO, 1999]. The size of each selected structural member is tabulated in Table 5, and the dynamic modal characteristics are shown in Table 6.

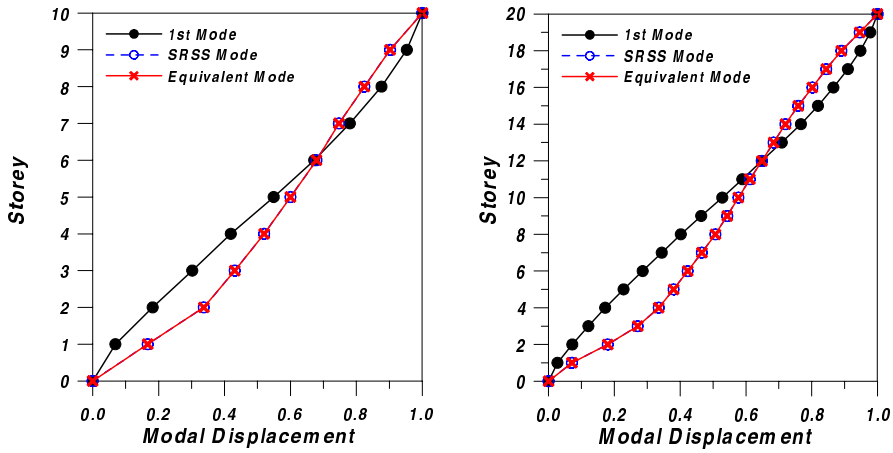

(a) 10-storey structure (b) 20-storey structure

Fig. 8. Mode shapes for evaluation of lateral loads.

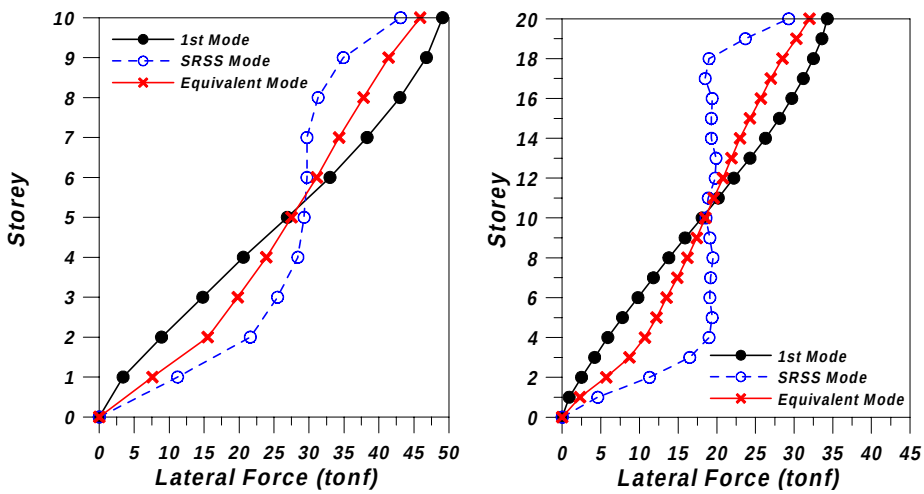

(a) 10-storey structure (b) 20-storey structure

Fig. 9. Lateral load patterns used in the pushover analysis.

Comparing the effective masses it can be noticed that the participation of higher modes is more significant in the 20-storey frame.

Figure 8 shows the mode shapes of the model structures obtained for the three patterns of lateral loads mentioned previously. It can be found that the SRSS and the equivalent mode shapes are almost identical, whereas the fundamental mode shape shows a little deviation from the others. Figure 9 indicates that the lateral loads resulting from the SRSS method are higher than those from the other methods in the lower stories but are smaller in the higher stories.

4.2. *Design spectrum and earthquake time history record*

Site-specific elastic design response spectrum, shown in Fig. 10(a), was constructed in accordance with Fig. 16-3 of UBC-97 with the seismic coefficients C_a and C_v

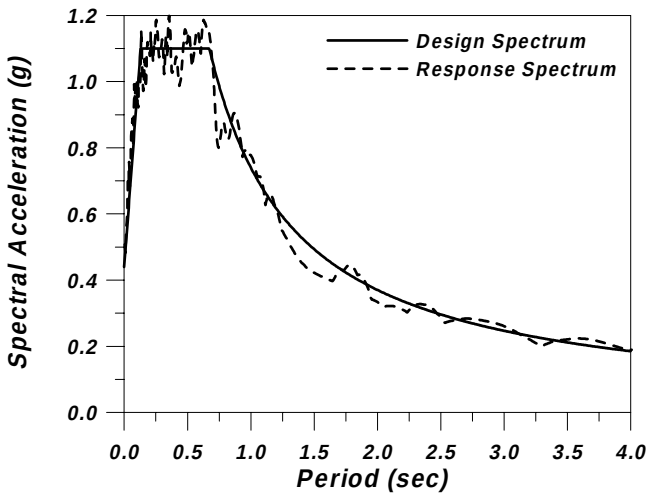

(a) Design and response spectra ($C_a = 0.44, C_v = 0.74$).

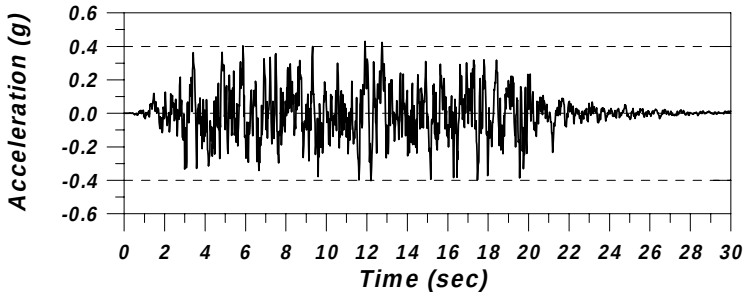

(b) Artifficial ground excitation

Fig. 10. Input seismic load.

as suggested in the Korean Seismic Design Guidelines II [Earthquake Engineering Society of Korea (EESK), 1997] for earthquakes with recurrence period of 2400 years on soil profile type (week soil). Based on the design spectrum time history record shown in Fig. 10(b) was generated using the program SIMQKE [Vanmarcke *et al.*, 1976] for comparison of the static procedure with the nonlinear dynamic THA. The response spectrum constructed from the time history record generated from the design spectrum is also plotted in Fig. 10(a), where it can be observed that the response spectrum matches well with the design spectrum.

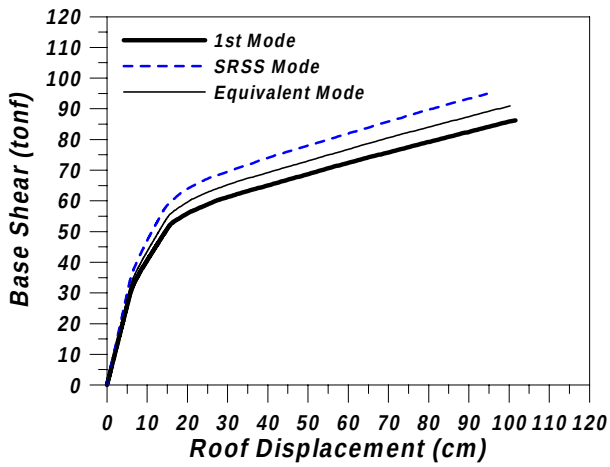

(a) Pushover curves

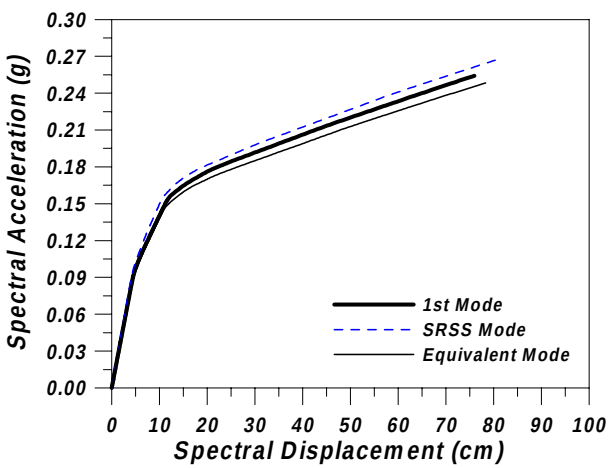

(b) Capacity spectra

Fig. 11. Formation of pushover curves and capacity spectra for each lateral load pattern (10-storey structure).

4.3. *Capacity spectrum*

The base shear-top storey displacement relationships (pushover curves) for the 10-storey model structure are shown in Fig. 11(a), which were obtained with the lateral static load gradually increased until the top storey displacement reached 4% of the total structure height. The pushover analysis was carried out using DRAIN-2D+ [Tsai *et al.*, 1997]. Then the force-displacement relationships were transformed into the capacity spectra of an equivalent SDOF system in ADRS format, which are plotted in Fig. 11(b).

4.4. *Evaluation of required supplemental damping*

The capacity spectrum and the demand spectra with various damping ratios were plotted simultaneously in ADRS format, and the performance points were evaluated. For comparison, nonlinear dynamic time history analyses were performed by DRAIN-2D+. It was assumed that hinge rotation takes place at the point-plastic hinge at element ends. Figures 12 and 13 represent the maximum storey and inter-storey drifts of the model structures obtained from the CSM and the THA. According to the results, the storey displacements of both structures computed from CSM slightly underestimate those obtained from THA. In the 10-storey structure, the results based on the fundamental mode shape are closest to the results from THA. However, in the 20-storey structure those based on the equivalent mode are closest, probably due to the participation of the higher modes. The comparison of Fig. 12(a) and Fig. 13(a) shows that the differences between the maximum storey displacements obtained from the CSM and the THA are larger in the 20-storey

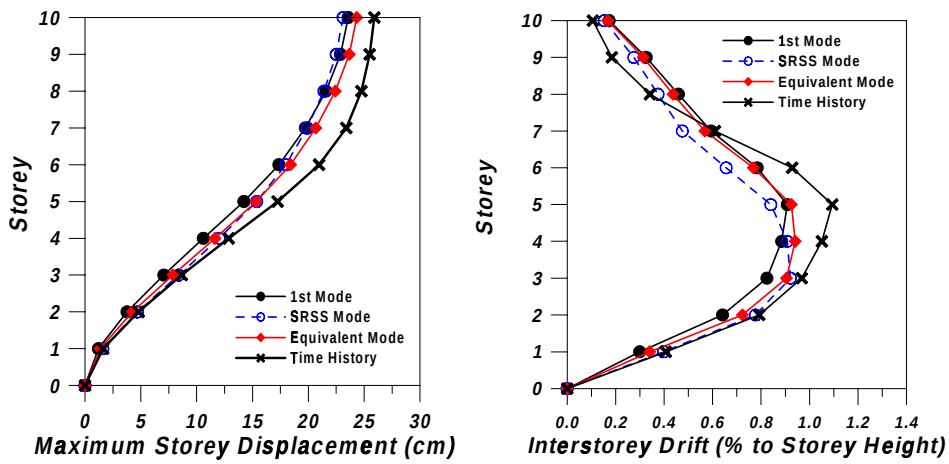

(a) Storey displacements (b) Inter-storey drifts

Fig. 12. Maximum storey and inter-storey drifts of the 10-storey model structure.

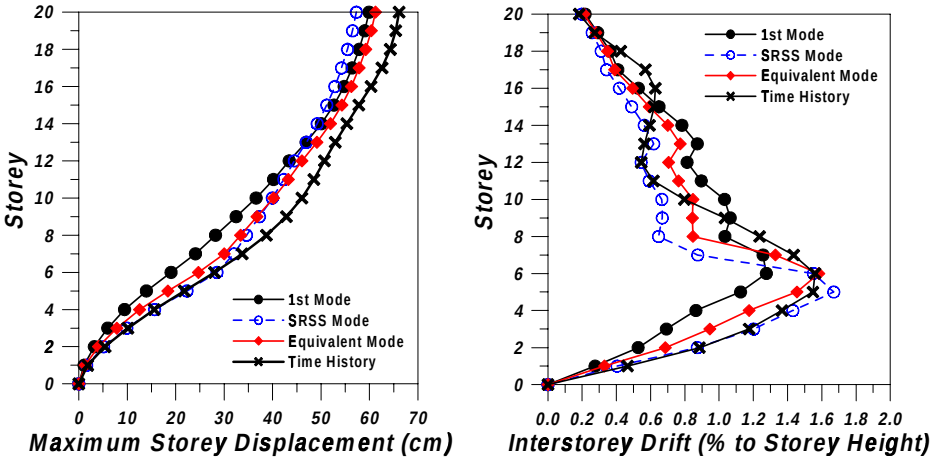

(a) Storey displacements (b) Inter-storey drifts

Fig. 13. Maximum storey and inter-storey drifts of the 20-storey model structure.

structure. It also can be observed that the CSM results considering higher modes are closer to those from the THA.

The inter-storey drifts indicate that for the given earthquake load both structures satisfy the collapse prevention limit state prescribed in the reference [EESK, 1997] which is the maximum inter-storey drift of 2.5% of the storey height, but that the *functional* limit states are not satisfied, which are 0.5% of the storey heights, except at the top two storeys. Therefore in this study the target roof displacements were set to be 0.5% of the structure height, which is 20 and 40 cm for the 10 and 20-storey model structures, respectively, and the required supplemental viscous damping ratios were estimated by the proposed method. To find out the amount of damping that should be provided by the dampers, the total required effective damping β_{eff} and the equivalent damping β_{eq} corresponding to the target displacements were obtained in the acceleration-displacement response spectra. Then the amount of the additional viscous damping ratios were computed using Eq. (2.7), and were presented in Table 7 together with the effective damping ratios and the elastic and the effective periods for each lateral loading pattern. It can be observed that to meet the same target displacement the methods utilising the equivalent mode and the SRSS mode result in the largest and the smallest required damping ratios, respectively.

4.5. *Distribution of supplemental viscous dampers*

The final step in the design process is to distribute the required supplemental damping throughout the storeys. Recognising that proper damper placement may affect its effectiveness significantly, many researchers have proposed variety of schemes for optimal damper placement. Zhang and Soong [1992] proposed a sequential

Table 7. Evaluation of the required damping for the different load patterns.

Model Structure	Load Patterns	T_e	T_{eff}	β_{eff} (%)	β_v (%)
10-storey	Fundamental Mode	1.65	1.87	31.4	10.6
	SRSS Mode	1.62	1.82	32.1	9.1
	Equivalent Mode	1.65	1.88	34.1	12.7
20-storey	Fundamental Mode	3.44	3.44	30.3	25.3
	SRSS Model	3.15	3.28	29.5	18.7
	Equivalent Mode	3.36	3.36	32.5	27.5

(T_e: elastic period, T_{eff}: effective period, β_{eff}: effective damping, β_v: required damping.)

optimisation procedure in which a performance index is maximised at each step to determine the optimal location of a single damper in each sequence. More recently, Wu *et al.* [1997] determined optimal damper locations considering inter-storey drifts and torsional responses. Also there are other methods based on optimal control theory [Loh *et al.*, 2000, for example]. Most of these schemes, however, were developed for structures deforming in linear elastic range. For structures that undergo inelastic deformation, the methods based on optimal control theory cannot be applied, and the sequential optimisation procedure may not be practical because of huge computational demand, especially in the stage of preliminary design.

In this study the dampers were distributed in each storey using Eq. (2.9), for which the storey-wise damper distribution pattern and the storey displacement shape need to be assumed. The following six cases were compared in the investigation. For each case the three lateral load patterns (fundamental mode, SRSS mode combination, and equivalent mode) were applied.

- Case 1: dampers are uniformly distributed in all storeys, and the displaced shape is proportional to the fundamental mode shape.
- Case 2: dampers are uniformly distributed in all storeys, and the displaced shape is proportional to the pushover curves.
- Case 3: damper size and displaced shape are proportional to the fundamental mode shape.
- Case 4: damper size and displaced shape are proportional to the pushover curve.
- Case 5: dampers are distributed proportionally to the inter-storey drifts, and displaced shape is proportional to the fundamental mode shape.
- Case 6: dampers are distributed proportionally to the inter-storey drifts, and the displaced shape is proportional to the pushover curve.

Table 8 presents the summation of damping coefficient of all the dampers distributed in each storey of the structure in accordance with the above six different distribution patterns. It can be observed that in both model structures the required viscous dampers are minimum in Case 6, which implies that the most efficient damper distribution scheme is to distribute them proportionally to the inter-storey drifts obtained from pushover curves. Table 8 also shows the ratio of

Table 8. Total amount of viscous damping distributed to each storey in accordance with the various methods.

(a) 10-storey structure

Distribution Patterns	Fundamental Model		SRSS Combination		Equivalent Mode	
	Sum. of Damping Coefficient (tonf-s/cm)	$\frac{D_{\max}}{D_{\mathrm{TG}}}$	Sum. of Damping Coefficient	$\frac{D_{\max}}{D_{\mathrm{TG}}}$	Sum. of Damping Coefficient (tonf-s/cm)	$\frac{D_{\max}}{D_{\mathrm{TG}}}$
Case 1	21.3	1.07	18.2	1.10	25.0	1.03
Case 2	20.8	1.08	19.1	1.09	25.5	1.03
Case 3	23.0	1.10	23.6	1.08	32.4	1.00
Case 4	23.4	1.10	23.4	1.09	29.7	1.05
Case 5	17.9	1.06	18.6	1.05	25.4	0.97
Case 6	16.0	1.08	14.8	1.10	18.9	1.05

(b) 20-storey structure

Distribution Patterns	Fundamental Model		SRSS Combination		Equivalent Mode	
	Sum. of Damping Coefficient (tonf-s/cm)	$\frac{D_{\max}}{D_{\mathrm{TG}}}$	Sum. of Damping Coefficient	$\frac{D_{\max}}{D_{\mathrm{TG}}}$	Sum. of Damping Coefficient (tonf-s/cm)	$\frac{D_{\max}}{D_{\mathrm{TG}}}$
Case 1	178.8	0.96	135.4	1.02	187.0	0.95
Case 2	180.8	0.96	145.8	1.00	204.4	0.93
Case 3	189.2	1.03	174.4	1.00	240.9	0.94
Case 4	212.4	1.01	208.4	0.98	266.1	0.95
Case 5	155.8	0.99	121.5	1.03	192.6	0.95
Case 6	138.2	1.02	87.6	1.10	141.2	1.01

($D_{\max}$: maximum displacement obtained from time history analysis, D_{TG}: target displacement.)

the maximum displacements obtained from the THA to the target displacements. It can be noticed that all the damper distribution patterns produce satisfactory results; in most cases the error is less than 10%. In the 10-storey structure, the maximum displacements resulted from applying the equivalent mode shape turned out to be closest to the target value. However, in the 20-storey structure, those for SRSS mode combination are most accurate in most cases. It also can be found that, in both model structures, SRSS pattern turned out to satisfy the performance objective with least amount of dampers in the Case 6, in which the dampers are distributed proportionally to the inter-storey drifts of the pushover curve.

Figure 14 describes the locations and sizes of plastic hinges before and after the dampers are installed in the 20-storey model structure in accordance with the damper distribution pattern of Cases 4 and 5. As expected, the size and the number of plastic hinge are greatly reduced after the dampers designed in accordance with the proposed method are installed. However, it can be observed that different patterns of damper distribution result in different location and size of plastic hinge, even though the maximum roof displacements are almost the same.

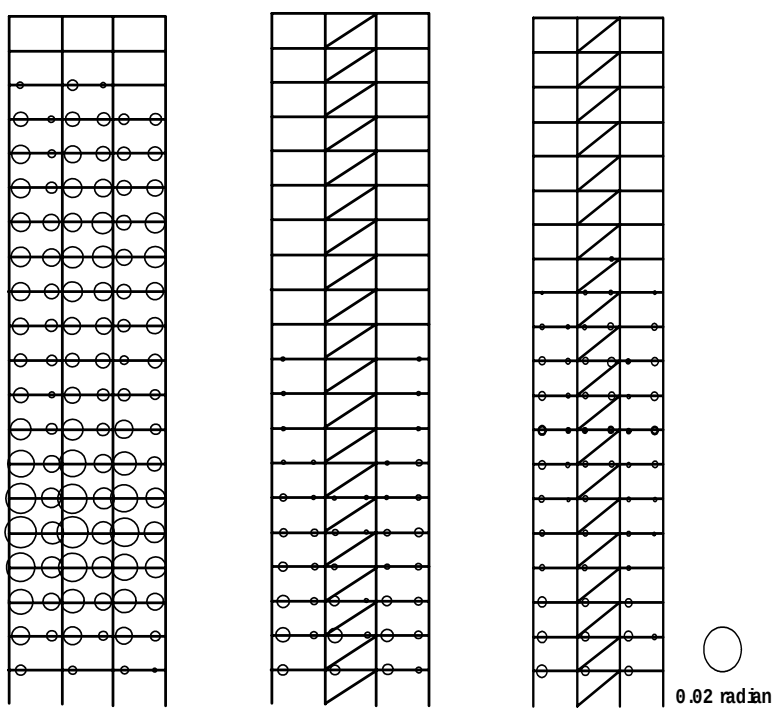

(a) No dampers (b) Case 4 distribution (c) Case 5 distribution

Fig. 14. Plastic hinge rotations and locations before and after the dampers are installed in the 20-storey model structure.

5. Conclusions

In this study a simple procedure was proposed using CSM to determine the amount of supplemental viscous damping required to limit the maximum response for a given earthquake level within a certain performance acceptance criteria. The proposed procedure was applied to SDOF systems with various natural periods, strain hardening ratios, ratio of yield strength to the strength demand in the corresponding linear system, to evaluate the applicability of the method in various conditions. It was also implemented to 10- and 20-storey framed structures by redistributing the required supplemental damping, estimated in an equivalent SDOF system, to each storey of the structure. The results were compared with those obtained from nonlinear dynamic time history analysis to evaluate the accuracy of the proposed method, which indicates that the proposed process is effective in the evaluation of supplemental damping required to meet the target performance criteria. In this sense the proposed process can be a potential tool for performance-based seismic design and retrofit of structures with supplemental viscous dampers. It should be pointed out, however, that the proposed design process may not be applicable where the assumptions and preconditions on which the CSM is based are not satisfied. Nevertheless it is expected that the proposed procedure may further expand the applicability of the CSM.

Acknowledgement

This research is funded by the Korea Science and Engineering Foundation under Grant No. R01-1999-00298. This financial support is gratefully acknowledged.

References

ATC [1996] Applied Technology Council, *Seismic Evaluation and Retrofit of Concrete Buildings, ATC-40*, Redwood City, California.

Chopra, A. K. [1995] *Dynamics of Structures: Theory and Applications to Earthquake Engineering*, Prentice Hall, Inc., Englewood Cliffs, New Jersey.

EESK [1997] Earthquake Engineering Society of Korea, *Seismic Design Guidelines II*, Ministry of Construction & Transportation, Seoul, Korea.

Fajfar, P. [2000] "A nonlinear analysis method for performance-based seismic design," *Earthq. Spectra* **16**(3), 573–592.

FEMA-274 [1997] Federal Emergency Management Agency, *NEHRP Guidelines for the Seismic Rehabilitation of Buildings*, Washington, D.C.

FEMA-274 [1997] Federal Emergency Management Agency, *NEHRP Commentary on the Guidelines for the seismic rehabilitation of buildings*, Washington, D.C.

Freeman, S. A. [1998] "Development and use of capacity spectrum method," *Proceedings of the 6th National Conference on Earthquake Engineering*, Seattle, Washington.

Freeman, S. A., Sasaki, K. and Paret, T. [1998] "Multi-mode pushover procedure — A method to identify the effects of higher modes in a pushover analysis," *Proceedings of the 6th National Conference on Earthquake Engineering*, Seattle, Washington.

Krawinkler, H. [1995] "New trends in seismic design methodology," *Proceeding the 10th European Conference on Earthquake Engineering*, Vienna.

Loh, C. H., Lin, P. Y. and Chung, N. H. [2000] "Design of dampers for structures based on optimal control theory," *Earthq. Engrg. Struct. Dyn.* **29**, 1307–1323.

Mahin, S. A. and Lin, J. [1983] *Inelastic Response Spectra for Single Degree of Freedom Systems*, Department of Civil Engineering, University of California, Berkeley.

POSCO Engineering & Construction Co., Ltd. [1999] *MIDAS-GEN, User's manual Vol. I–Vol. IV*, POSCO Engineering & Construction Co., Ltd., Seoul, Korea.

Soong, T. T. and Dargush, G. F. [1997] *Passive Energy Dissipation Systems in Structural Engineering*, John Wiley & Sons, Inc., New York.

Tsai, K. C. and Li, J. W. [1997] "DRAIN2D+, A general purpose computer program for static and dynamic analyses of inelastic 2D structures supplemented with a graphic processor," *Report No. CEER/R86-07*, National Taiwan University, Taipei, Taiwan.

Tsopelas, P., Constantinou, M. C., Kircher, C. A. and Whittaker, A. S. [1997] "Evaluation of simplified method of analysis for yielding structures," *Technical Report NCEER-97-0012*, National Center for Earthquake Engineering Research, State University of New York at Buffalo.

Valles, R. E., Reinhorn, A. M., Kunnath, S. K., Li, C. and Madan, A. [1996] "IDARC 2D version 4.0: A computer program for the inelastic damage analysis of buildings," *Technical Report NCEER-96-0010*, National Center for Earthquake Engineering Research, State University of New York at Buffalo.

Vanmarcke, E. H. and Gasparini, D. A. [1976] *A Program for Artificial Motion Generation, User's Manual and Documentation*, Department of Civil Engineering, Massachusetts Institute of Technology.

Wu, B., Ou, J. P. and Soong, T. T. [1997] "Optimal placement of energy dissipation devices for three-dimensional structures," *Engrg. Struct.* **19**(2), 113–125.

Zhang, R. H. and Soong, T. T. [1992] "Seismic design of viscoelastic dampers for structural applications," *ASCE J. Struct. Engrg.* **118**(5), 1375–1392.